# Optimal electromagnetic-wave absorption by enhanced dipole polarization in Ni/C nanocapsules

Han Wang, Huaihong Guo, Yingying Dai, Dianyu Geng, Zheng Han et al.

## Related Articles

Neuronal alignment on asymmetric textured surfaces
Appl. Phys. Lett. 101, 143701 (2012)

Anomalous behavior of epitaxial indium nano-contacts on cadmium-zinc-telluride
Appl. Phys. Lett. 101, 132108 (2012)

Control of nanocrystal surface defects for efficient charge extraction in polymer-ZnO photovoltaic systems
J. Appl. Phys. 112, 066103 (2012)

Experimental surface-enhanced Raman scattering response of two-dimensional finite arrays of gold nanopatches
Appl. Phys. Lett. 101, 111606 (2012)

Nano-hillock formation in diamond-like carbon induced by swift heavy projectiles in the electronic stopping regime: Experiments and atomistic simulations
Appl. Phys. Lett. 101, 113115 (2012)

## Additional information on Appl. Phys. Lett.

Journal Homepage: http://apl.aip.org/

Journal Information: http://apl.aip.org/about/about_the_journal

Top downloads: http://apl.aip.org/features/most_downloaded

Information for Authors: http://apl.aip.org/authors

# Optimal electromagnetic-wave absorption by enhanced dipole polarization in Ni/C nanocapsules

Han Wang, Huaihong Guo, Yingying Dai, Dianyu Geng, Zheng Han, Da Li, Teng Yang,[a]
Song Ma,[b] Wei Liu, and Zhidong Zhang
*Shenyang National Laboratory for Materials Science, Institute of Metal Research, and International Centre for Materials Physics, Chinese Academy of Sciences, 72 Wenhua Road, Shenyang 110016, People's Republic of China*

Electromagnetic-wave (EMW) absorption by Ni/C nanocapsules with similar permeability but different permittivity mainly due to differences in the graphite-shell thickness has been investigated. The optimal working frequency could appear at S-band and C-band and considerable strong EMW absorption was achieved. For the optimal Ni/C nanocapsules, a reflection loss exceeding $-20$ dB was reached from 2.6 to 8.2 GHz with a maximum value of $-40$ dB at 3 GHz. The improved absorption can be attributed to an optimal electromagnetic match and an enhanced dipole polarization upon increasing of shell thickness. © 2012 American Institute of Physics. [http://dx.doi.org/10.1063/1.4747811]

Recently, much research has been focused on core/shell nanostructures (dielectric shells and magnetic nanoparticles as cores) as electromagnetic-wave (EMW) absorbing materials.[1–9] The nanoshell not only protects the magnetic nanostructures against oxidation or corrosion[2,4,10] but also improves the impedance match between the magnetic and dielectric components in the core/shell structure which enhances the EMW absorption.[4,6,8] The metallic soft-magnetic material of the cores is important for their micro-wave absorption at higher than gigahertz frequencies, which is due to the higher Snoek limit.[1,4,11] Among the core/shell structures, Ni-based EMW absorbing nanocomposites, such as Ni/ZnO,[8] Ni/SiO$_2$,[12] Ni/polyaniline,[9] Ni/C,[13] and Ni/carbon nanotubes,[14,15] have drawn widespread attention lately. Ni/graphite[13–15] takes a special position, because the graphite shell has excellent dielectric properties, these composites are cheap, they have low density, and are more environment-friendly than other dielectric materials.[2,4,13] However, the existing nanocapsules only display good absorption at one particular high frequency, such as Ni/PANi (Ref. 9) at 17 GHz and Ni/C (Ref. 13) at 13 GHz.

The important question how the shell affects the EMW absorption is still not answered, and it is a challenge to find out whether there is a shell thickness at which optimal absorption can be achieved. In this letter, we present improved EMW performance of Ni/C nanocapsules than previous reported Ni/C and have investigated the electro-magnetic properties of core/shell structures with variable shell thickness, which may help to solve the above puzzles and promote the application and development of EMW-absorption materials.

Ni/C nanocapsules[16] with different average shell thickness were prepared by modified arc-discharging[8] with introduction of 5, 10, and 35 ml ethanol (C$_2$H$_5$OH) as the carbon source into the reaction chamber (volume: 70 l) and the cor-

responding nanocapsule samples are marked as samples S$_1$, S$_2$, and S$_3$, respectively. The TEM image in Fig. 1(a) shows a diameter distribution of 30–80 nm and an average diameter of 50 nm. The HRTEM images in Figs. 1(b)–1(d) indicate that the samples S$_1$, S$_2$, and S$_3$ have distinct characteristics of the core/shell structure and a close view of the core in the inset of Fig. 1(b) indicates a distance of 0.203 nm of (111) planes of the face-centered-cubic (FCC) Ni in the core. The x-ray diffraction patterns (not shown here) point out that the cores of the capsules consist of FCC Ni and no nickel oxides or nickel carbides are found. In the inset of Fig. 1(c), a zoom-in of the shell structure gives a distance of 0.335 nm between two closest planes along the [0001] direction—a fingerprint of graphite. The thickness of the graphite shell of
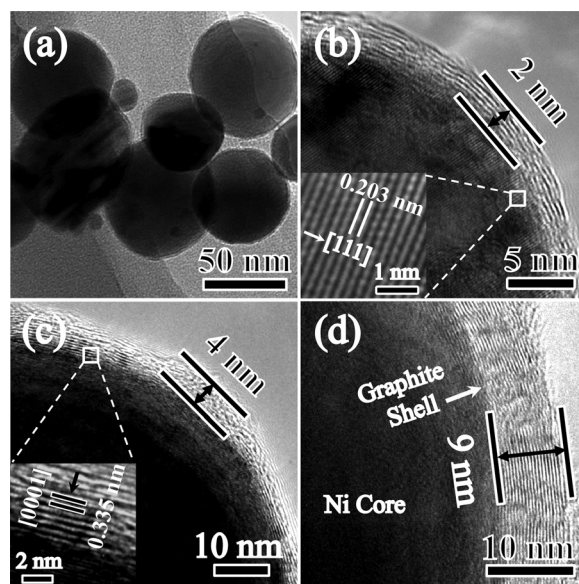


FIG. 1. Microstructure of Ni/C nanocapsules. (a) TEM image of sample S$_1$ and (b)–(d) HRTEM images of samples S$_1$, S$_2$, and S$_3$ with graphite shell thicknesses of 2 nm, 4 nm, and 9 nm, respectively. The insets of (b) and (c) show HRTEM images of the Ni core and the graphite shell.

a)yangteng@imr.ac.cn.
b)songma@imr.ac.cn.

the nanocapsules gradually increases from 2 nm for sample $S_1$ to 4 nm and 9 nm for samples $S_2$ and $S_3$, respectively.

The average thickness of the nanocapsules in each sample was determined by thermal gravimetric analysis (TGA) and differential scanning calorimetry (DSC) at ambient pressure from 100 °C to 800 °C with a heating rate of 10 °C/min. The results for the samples $S_1$ and $S_3$ are shown in Figs. 2(a) and 2(b), respectively. Both samples display three stages of oxidation behavior: the first stage (250–280 °C) is associated with gradual weight gain due to oxidation of the graphite shells and of a small quantity of Ni nanoparticles not well coated with graphite. The second stage (280–320 °C) is the oxidation of the Ni cores after oxidation of the graphite shells. In the third stage (320–450 °C), Ni cores initially very well coated with graphite shells are oxidized. The difference between both samples is at the temperature position and in the width of the DSC peaks. Basically, thicker coating enhances the protection against oxidation in the same environment and at the same temperature-change rate. The two prominent DSC peaks shift about 20 to 30 °C to higher temperatures and the peak for $S_3$ is wider than for $S_1$, indicating that the average thickness of the graphite shell is larger in $S_3$,[2] which is consistent with the direct observation by HRTEM. The magnetic hysteresis loops of the three samples (measured at 295 K in a superconducting quantum interference device) are shown in Fig. 2(c). It is found that the Ni cores in the three samples have very similar magnetic properties, which is consistent with the permeability results in



FIG. 3. (a)–(c) Frequency dependence of RL of $S_1$, $S_2$, and $S_3$ for different values of the thickness d of the absorbing layer and (d) comparison of the match frequency and RL values of $S_1$, $S_2$, and $S_3$ at different d values.

Fig. 4(c). As a result, the difference of the graphite-shell thickness is the largest difference between the three samples.

The frequency dependence of the reflection loss (RL) has been derived by applying transmission-line theory[17] to the measured complex permittivity $\varepsilon_r (\varepsilon_r = \varepsilon' - j\varepsilon'')$ and permeability $\mu_r (\mu_r = \mu' - j\mu'')$ of samples consisting of 40 wt. % Ni/C nanocapsules uniformly mixed with wax.[4] Using the densities of wax and of nickel, the volume fraction of nanocapsules was estimated to be 55%. Figure 3 shows that all of the nanocapsules $S_1$, $S_2$, and $S_3$ exhibit excellent performance. By choosing an appropriate absorbing-layer thickness d between 3.8 and 8.8 mm, for all samples RL values exceeding −10 dB (90% EMW absorption) are obtained in the whole frequency range of 2–18 GHz. Figure 3(d) shows that an increase of the shell thickness $t_{shell}$ at fixed d not only brings about a red shift of the frequency of the RL peaks but also an increase of the RL peak values. As shown in Fig. 3(c), in the frequency range from 2.6 GHz to 8.2 GHz, RL values of $S_3$ exceeding −20 dB (99% EMW absorption) can always be achieved by selecting a proper layer thickness d. The maximum value of RL of $S_3$ is found to be −40 dB at a low frequency of 3 GHz. By changing the graphite-shell thickness, the optimal working frequency of the samples, compared with previous results[13] (occurring at 13 GHz), has shifted from Ku-band (12–18 GHZ) to S-band (2–4 GHz) and C-band (4–8 GHz). This suggests that, more than $S_1$ and $S_2$, sample $S_3$ is an attractive candidate for EMW absorber.
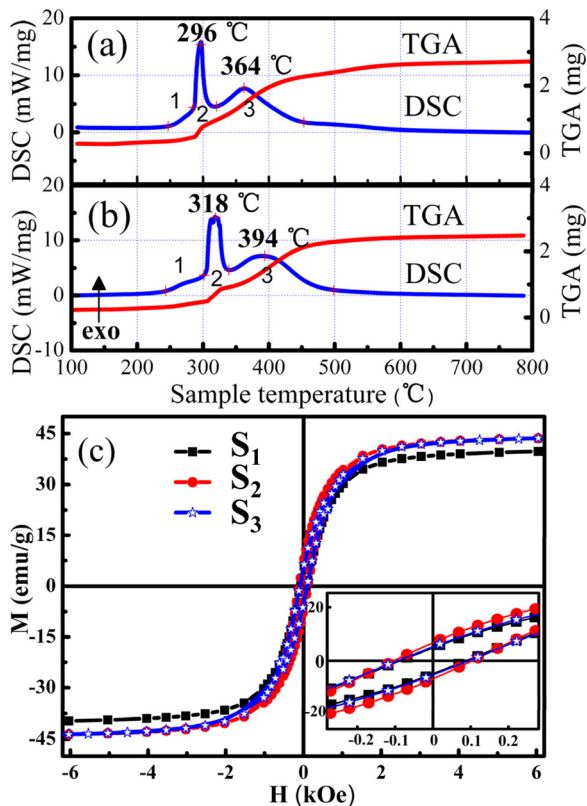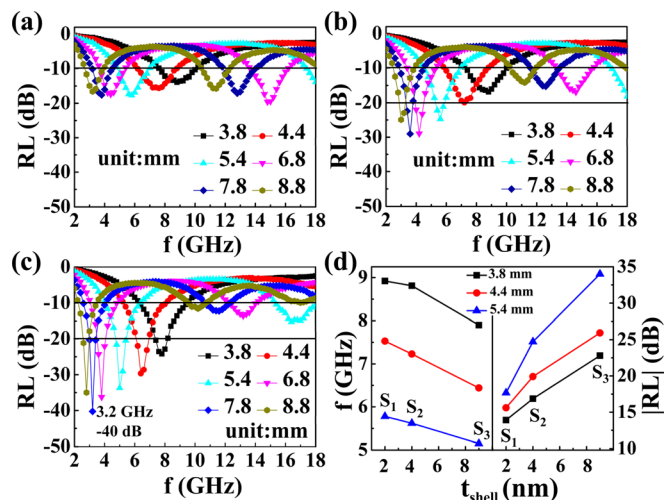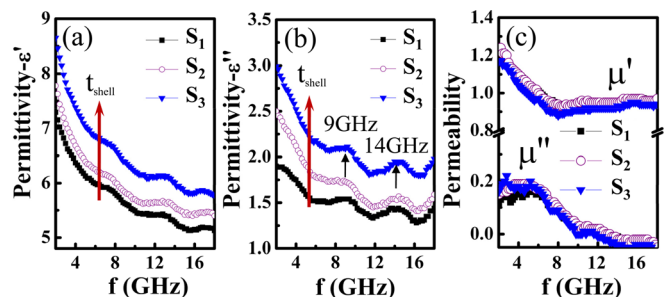


FIG. 2. Ensemble average of both the shell thickness and the core magnetism of Ni/C nanocapsules. (a) and (b) DSC (blue line) and TGA (red line) curves of the samples $S_1$ and $S_3$, and (c) magnetic hysteresis loops at 295 K for samples $S_1$–$S_3$, showing similar magnetic properties of the Ni core.



FIG. 4. Permittivity $\varepsilon$ and permeability $\mu$ of the samples $S_1$, $S_2$, and $S_3$. (a) and (b) Frequency dependence of the real and imaginary parts of $\varepsilon$ and (c) frequency dependence of the real and imaginary parts of $\mu$.

Figures 4(a) and 4(b) show the frequency dependencies of $\varepsilon'$ and $\varepsilon''$ for all samples. Both $\varepsilon'$ and $\varepsilon''$ display a similar tendency of decreasing with the frequency increasing from 2 to 18 GHz which is due to increased lagging behind of the dipole-polarization response with respect to the electric-field change at higher frequencies.[18] In addition, there are two clear resonance peaks around 9 GHz and 14 GHz for all three samples, which may be attributed to interfacial polarization resonance due to the electronegativity difference between the Ni core and the graphite shell[8,13] and to permanent electric dipoles resulting from defects in the graphite shell.[5,9] Dong *et al.* have observed an enhanced polarization loss but an irregular dipole polarization with increasing contents of PANi in Ni/PANi systems.[9] Li *et al.* have reported enhanced dielectric polarization but an almost unchanged dielectric loss with increasing volume concentration of $Co_2Z$ barium ferrite in $Co_2Z$ barium ferrite/epoxy.[19] However, in contrast with the Ni/PANi and $Co_2Z$ barium ferrite/epoxy systems, the Ni/C systems show a simultaneous increase of the dipole polarization and the polarization loss, causing that both $\varepsilon'$ and $\varepsilon''$ clearly increase in the sequence $S_1$, $S_2$, and $S_3$. The simultaneous increase of $\varepsilon'$ and $\varepsilon''$ shows excellent core/shell structures of the Ni/C nanocapsules compared with Ni/PANi and $Co_2Z$/epoxy nanocomposites. Compared to the distinct variation of $\varepsilon_r$, there is no clear difference between the $\mu_r$ values of the different samples and the permeability curves almost coincide (Fig. 4(c)). As a result, the improvement of the RL values for $S_3$ is ascribed to the simultaneous increase of the dipole polarization and the polarization loss of the nanocapsules $S_3$ due to a bigger shell thickness.

The gradual increase of $\varepsilon'$ and $\varepsilon''$ from $S_1$ to $S_3$ is clearly due to the increasing thickness of the graphite shell, which will be further illustrated by the following analysis based on basic electrodynamics theory and the Bruggeman theory.[22,23] The electric-dipole moments of the core/shell structure in the matrix can be mimicked by a homogeneous structure[20,21] (shown in the inset of Fig. 5) in which the permittivities $\varepsilon_1$ and $\varepsilon_2$ are represented by $\gamma\varepsilon_1$, with $\gamma = [\beta(1 + 2\beta) + 2\alpha\beta(1 - \beta)]/[(1 + 2\beta) - \alpha(1 - \beta)]$ in which $\beta = \varepsilon_2/\varepsilon_1$ and $\alpha = (R_1/R_2)^3 = (R_1/(R_1 + t_{shell}))^3$. According to the TEM images $R_1 = 50$ nm. Using the Bruggeman theory, one obtains[22,23]

$$\frac{V}{\alpha}\frac{\gamma\varepsilon_1 - \varepsilon_{eff}}{\gamma\varepsilon_1 + 2\varepsilon_{eff}} + \left(1 - \frac{V}{\alpha}\right)\frac{\varepsilon_m - \varepsilon_{eff}}{\varepsilon_m + 2\varepsilon_{eff}} = 0, \qquad (1)$$
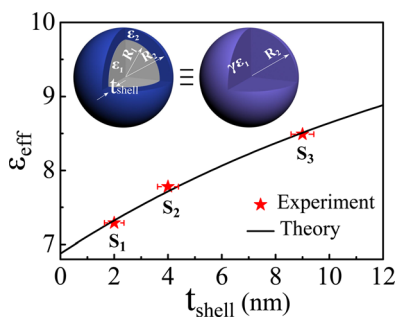


FIG. 5. Increase of the permittivity with increasing thickness of the graphite shell. The solid line represents a fit to the experimental data (red star with error bar) based on the Bruggeman theory. The inset shows the uniform structure that mimics the Ni/C nanocapsule core/shell structure.

where $V$ is the volume fraction of the nanocapusles and $\varepsilon_m$ ($= 2.2$) is the permittivity of the wax matrix. From Eq. (1), we get

$$-2\varepsilon_{eff}^2 + \varepsilon_{eff}\left[\gamma\left(3\frac{V}{\alpha} - 1\right)\varepsilon_1 + \left(2 - 3\frac{V}{\alpha}\right)\varepsilon_m\right] + \gamma\varepsilon_1\varepsilon_m = 0. \qquad (2)$$

By means of Eq. (2), the effective permittivity $\varepsilon_{eff}$ can be calculated as a function of $t_{shell}$. We have fitted the experimental data to Eq. (2) with $\varepsilon_1$ and $\varepsilon_2$ as fitting parameters. The fit represents the experimental data quite well with $\varepsilon_{eff}$ monotonously increasing with increasing $t_{shell}$. The obtained fitting parameters, $\varepsilon_1 = 10$ and $\varepsilon_2 = 18$, are around 10%–20% larger than the experimental bulk values. This increased permittivity of the nanocapsules with respect to values for the bulk materials is very likely a size effect. A similar increase has been reported upon going from bulk graphite to carbon tubular nanostructures and nanocapsules.[24–26]

We have seen that an increase of $t_{shell}$ is accompanied by an increase of $\varepsilon_{eff}$. However, this does not guarantee a better EMW performance because a proper match between the dielectric and magnetic properties is the key factor in optimizing EMW absorption.[2,6,9] As a matter of fact, in other Ni/C systems,[13] for $t_{shell}$ larger than 10 nm, an RL value exceeding −20 dB appears only at one frequency (13 GHz). Therefore, the shell thickness of 9 nm is almost optimal for the best EMW absorption by Ni/C nanocapsules.

In conclusion, a series of Ni/C EMW absorbing nanocapsules with similar permeability of the core, but different permittivity, mainly due to differences in the thickness of the graphite shell have been prepared. By varying the thickness of the shell of Ni/C nanocapsules, the optimal working frequency with adequate EMW absorption can be shifted from high frequency band (Ku band) to low frequency band (S-band and C-band). RL values exceeding −20 dB (99% EMW absorption) can be reached from 2.6 GHz to 8.2 GHz and a maximum value of RL as large as −40 dB is obtained at about 3 GHz. This optimal EMW absorption is ascribed to an increase of the dipole-polarization and the polarization loss caused by an increase of the thickness of the graphite shell of the Ni/C nanocapsules.

[1]V. B. Bregar, IEEE Trans. Magn. **40**, 1679 (2004).
[2]R. C. Che, L. M. Peng, X. F. Duan, Q. Chen, and X. L. Liang, Adv. Mater. **16**, 401 (2004).
[3]F. Qin and C. Brosseau, J. Appl. Phys. **111**, 061301 (2012).
[4]Z. Han, D. Li, H. Wang, X. G. Liu, J. Li, D. Y. Geng, and Z. D. Zhang, Appl. Phys. Lett. **95**, 023114 (2009).
[5]P. C. P. Watts, W. K. Hsu, A. Barnes, and B. Chambers, Adv. Mater. **15**, 600 (2003).
[6]L. G. Yan, J. B. Wang, X. H. Han, Y. Ren, Q. F. Liu, and F. S. Li, Nanotechnology **21**, 095708 (2010).
[7]X. Li, Z. Wang, Y. L. Zuo, and X. N. Shi, Nanotechnology **22**, 045707 (2011).

[8]X. G. Liu, J. J. Jiang, D. Y. Geng, B. Q. Li, Z. Han, W. Liu, and Z. D. Zhang, Appl. Phys. Lett. **94**, 053119 (2009).

[9]X. L. Dong, X. F. Zhang, H. Huang, and F. Zuo, Appl. Phys. Lett. **92**, 013127 (2008).

[10]P. Lukanov, V. K. Anuganti, Y. Krupskaya, A. M. Galibert, B. Soula, C. Tilmaciu, A. H. Velders, R. Klingeler, B. Buchner, and E. Flahaut, Adv. Funct. Mater. **21**, 3583 (2011).

[11]P. Toneguzzo, G. Viau, O. Acher, F. Fievet-Vincent, and F. Fievet, Adv. Mater. **10**, 1032 (1998).

[12]K. Peng, L. P. Zhou, A. P. Hu, Y. H. Tang, and D. Li, Mater. Chem. Phys. **111**, 34 (2008).

[13]X. F. Zhang, X. L. Dong, H. Huang, Y. Y. Liu, W. N. Wang, X. G. Zhu, B. Lv, J. P. Lei, and C. G. Lee, Appl. Phys. Lett. **89**, 053115 (2006).

[14]T. N. Narayanan, V. Sunny, M. M. Shaijumon, P. M. Ajayan, and M. R. Anantharaman, Electrochem. Solid-State Lett. **12**, K21–K24 (2009).

[15]F. S. Wen, H. B. Yi, L. Qiao, H. Zheng, D. Zhou, and F. S. Li, Appl. Phys. Lett. **92**, 042507 (2008).

[16]Z. D. Zhang, J. Mater. Sci. Technol. **23**(01), 1–14 (2007).

[17]Y. Naito and K. Suetake, IEEE Trans. Microwave Theory Tech. **19**, 65 (1971).

[18]K. C. Kao, *Dielectric Phenomena in Solids* (Elsevier, New York, 2004), Chap. 2, pp. 86–94.

[19]Z. W. Li, G. Q. Lin, and L. B. Kong, IEEE Trans. Magn. **44**, 2255 (2008).

[20]J. W. Haus, H. S. Zhou, S. Takami, M. Hirasawa, I. Honma, and H. Komiyama, J. Appl. Phys. **73**, 1043 (1993).

[21]J. D. Jackson, *Classical Electrodynamics* (John Wiley & Sons, Inc., New York, 1962), Chap. 1, p. 48.

[22]D. Stroud, Phys. Rev. B **12**, 3368 (1975).

[23]C. Brosseau, J. Phys. D: Appl. Phys. **39**, 1277 (2006).

[24]P. C. P. Watts, D. R. Ponnampalam, W. K. Hsu, A. Barnes, and B. Chambers, Chem. Phys. Lett. **378**, 609 (2003).

[25]X. F. Zhang, X. L. Dong, H. Huang, D. K. Wang, B. Lv, and J. P. Lei, Nanotechnology **18**, 275701 (2007).

[26]J. Wu and L. Kong, Appl. Phys. Lett. **84**, 4956 (2004).